Chromatographic Estimation of Drug Disposition Properties by Means of Immobilized Artificial Membranes (IAM) and C18 Columns

Elisabet Lázaro,[†] Clara Ràfols,[†] Michael H. Abraham,[‡] and Martí Rosés*,[†]

Departament de Química Analítica, Universitat de Barcelona, Martí i Franquès 1, E-08028 Barcelona, Spain, and Department of Chemistry, University College London, 20 Gordon Street, London WC1H 0AJ, U.K.

Received February 23, 2006

Chromatographic retention measurement in immobilized artificial membranes (IAMs) is considered a fast and reliable method to predict biological properties (drug distribution) because of the IAM structure, which consists of phospholipid analogues bonded covalently to silica particles. A new parameter (*d*) is proposed to estimate the similarity between IAM columns, conventional HPLC columns, and drug distribution systems, and thus the performance of chromatographic systems to predict drug distribution. An IAM.PC.DD2 column has been used for this study, together with two XTerra columns (MSC18 and RP18), at several acetonitrile−water mobile phases. According to the *d* parameter, good correlations should be obtained between chromatographic systems (both IAM and C18) and octanol−water partition coefficient (log *P*), and thus both types of columns could be used to obtain log *P* values. The IAM.PC.DD2 system shows a close similarity to human skin partition, tadpole narcosis, and blood−brain permeability processes, showing that it can be useful as a model for these biological processes. Controversially, it is shown that human skin permeation is more similar to C18 partition than to IAM partition. Other biological processes such as blood−brain distribution and tissue−blood partition show a poor similarity to IAM and C18 systems, demonstrating that estimation of these drug distribution processes by chromatographic measurements may not be adequate.

Introduction

Drug distribution and activity depend on interactions with biological membranes, so the evaluation of these interactions is a key issue in the drug discovery process. Partition coefficients between an aqueous phase and a lipid phase are thought to predict the drug transport across biological membranes. As an example, the logarithm of octanol−water partition coefficient (log *P*)[1] and the logarithm of the partition coefficient in liposome systems (log P_{SUV})[2,3] have been tested. Since drug distribution prediction by means of these techniques may be experimentally laborious, there is a need for faster predictive models. In this sense, there have been different approaches, such as biosensors[4] or IAM (immobilized artificial membranes) chromatography.

IAMs were introduced as HPLC column-packing materials by Pidgeon and Venkataram.[5] The IAMs are prepared by linking covalently synthetic phospholipid analogues to silica−propylamine particles to mimic the lipid environment of a fluid cell membrane on a solid matrix. The goal was to get fast and accurate predictions of drug distribution in biological systems directly from the HPLC retention measurements. Several correlations between IAM chromatography and biological systems have been published. Pidgeon et al.[6] observed a weak correlation of the IAM retention factor logarithm (log k_{IAM}) with rat intestinal absorption ($r = 0.791$) and with permeability through Caco-2 cells ($r = 0.762$) for structurally different drugs, but they improved correlations by means of a molecular weight correction ($r = 0.858$ and $r = 0.854$, respectively). Nasal et al.[7] found a good correlation ($r = 0.942$) between log k_{IAM} and skin permeability coefficients (log K_p) for a set of 10 steroids. However, they obtained a poorer correlation ($r = 0.765$) for a set of 14 phenolic compounds. Barbato et al.[8] showed a good correlation ($r = 0.952$) of log k_{IAM} with the activity data on closed sodium channels for a set of 13 anaesthetics, after removing two outliers. The retention factors on IAM showed poor correlation ($r = 0.576$) with the blood−brain concentration ratios (log BB) in the study by Salminen et al.[9] using 26 structurally different drugs. When they took into account the effect of ionization and solute size and removed five outliers, the regression model was improved ($r = 0.921$). Reichel and Begley[10] studied the correlation between the log k_{IAM} and the logarithm of brain uptake index (log BUI) for six steroids ($r = 0.854$) and six biogenic amines ($r = 0.864$). A good correlation ($r = 0.91$) of log k_{IAM} with rat passive intestinal permeability (P_a) was observed for a set of 12 structurally diverse drugs, with molar volume as an additional descriptor, in the study by Genty et al.[11] The relation between IAM binding data (CHI IAM) of known drug molecules and human serum albumin (HSA) binding, both obtained by chromatography, was studied by Valko et al.,[12] showing that compounds with a certain lipophilicity bind to both membrane and HSA.

The main purpose of this work is to characterize an IAM column by means of the solvation parameter model and to study its similarity with common C18 chromatographic (Waters XTerra columns) and biological (blood−brain distribution, intestinal absorption, skin permeability, and partition ...) systems. According to these similarities, we can choose the most suitable systems (IAM or C18) in order to estimate biological properties by means of chromatographic measures.

Theoretical Basis

Biological activities of solutes can be related to structural descriptors by means of quantitative structure−activity relationships (QSARs). Among the QSAR models, the solvation parameter model[13,14] has successfully described many biologi-

* To whom correspondence should be addressed. Phone: +34934039275. Fax: +34934021233. E-mail: marti@apolo.qui.ub.es.
[†] Universitat de Barcelona.
[‡] University College London.

10.1021/jm0602108 CCC: $33.50
Published on Web 07/19/2006

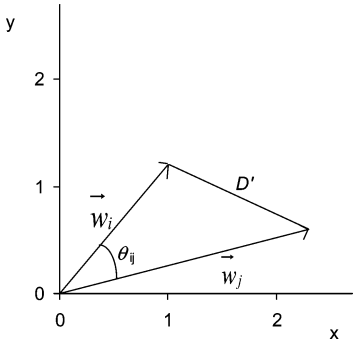

Figure 1. Schematic representation in two dimensions (only two coefficients) of LSER vectors, showing the angle θ_{ij} and the distance D' between them.

cally interesting processes as well as physicochemical ones. For instance, this model was used to characterize the octanol−water partition (log P),[15] tadpole narcosis (1/log C_{nar}),[16] skin permeation and partition (log K_p and log K_{sc}),[17] drug transport across the blood−brain barrier (log BBB),[18,19] human intestinal absorption,[20−22] tissue−blood partition,[23,24] micellar electrokinetic chromatography (MEKC),[25−28] and reversed-phase liquid chromatography (RPLC)[29−31] processes.

This solvation parameter model, the linear free energy relationship (LFER), can be written as

$$\mathrm{SP} = c + eE + sS + aA + bB + \upsilon V \tag{1}$$

where SP is the dependent solute property. The solute descriptors are the excess molar refraction E, the dipolarity/polarizability S, the solute's effective hydrogen-bond acidity A and hydrogen-bond basicity B, and McGowan's characteristic volume V.

When SP is the chromatographic retention factor (as log k), the coefficients in eq 1, which are calculated by multiple linear regression, represent the difference in solvation properties of both phases forming the chromatographic system. Coefficient e depends on the difference in the capacity of the solvated stationary and mobile phases to interact with solute n- or π- electrons; s is a measure of the difference in the capacity of the solvated phases to take part in dipole−dipole and dipole−induced dipole interactions; coefficients a and b represent the differences in hydrogen-bond basicity and acidity, respectively, between the stationary and the mobile phases; and υ is a measure of the relative ease of forming a cavity for the solute in the solvated stationary and mobile phases.

Since the same eq 1 can be applied to biological and physicochemical processes, it should be possible to find correlations between both kinds of processes. Since the solvation parameter model, as many QSAR and chromatographic models, can only characterize drug passive transport processes, the correlations are restricted to these kind of processes. Active transport processes, such as protein transport, cannot be modeled well by eq 1, and thus they are not considered in our approach. To test if a physicochemical process can model a biological process, it is useful to study the relation between their LFER coefficients. Ishihama and Asakawa[32] considered these coefficients as components of a vector in five dimensional (coefficients) space and proposed cos θ_{ij} as a measure of the similarity of the two LFERs, θ_{ij} being the angle between the two LFER vectors ($\vec{w}_i$ and $\vec{w}_j$) (see Figure 1). If the two systems are mathematically similar, the value of cos θ_{ij} becomes close to 1. The cos θ_{ij} can be calculated as follows:

$$\cos\theta_{ij} = \frac{\vec{w}_i \cdot \vec{w}_j}{|\vec{w}_i||\vec{w}_j|} = \frac{e_i e_j + s_i s_j + a_i a_j + b_i b_j + \upsilon_i \upsilon_j}{\sqrt{e_i^2 + s_i^2 + a_i^2 + b_i^2 + \upsilon_i^2}\sqrt{e_j^2 + s_j^2 + a_j^2 + b_j^2 + \upsilon_j^2}} \tag{2}$$

Later, Abraham[17,33] compared different systems by means of the distance (D') between them (see Figure 1). He considered the five coefficients of any system as a point in five-dimensional space and calculated the distance between each two points, suggesting that D' should be less than about 0.5−0.8 if the systems are chemically similar.

We proposed to use the distance between the normalized vectors of the systems as another measure of the similarity of these systems.[34] The LFER system can be written in matrix or vectorial notation as

$$\mathrm{SP} = c + (e\ s\ a\ b\ \upsilon)\begin{pmatrix} E \\ S \\ A \\ B \\ V \end{pmatrix} \tag{3}$$

or

$$\mathrm{SP} = c + \vec{w}\vec{W} \tag{4}$$

where $\vec{w}$ is the coefficients vector and $\vec{W}$ the solute descriptors vector. The coefficients vector can be normalized ($\vec{w}_u$) by the following equations:

$$\vec{w} = l\vec{w}_u \tag{5}$$

$$\vec{w}_u = \frac{1}{l}(e\ s\ a\ b\ \upsilon) \tag{6}$$

$$l = \sqrt{e^2 + s^2 + a^2 + b^2 + \upsilon^2} \tag{7}$$

where l is the length of the coefficients vector.

If there are two different systems with $\vec{w}_{ui}$ and $\vec{w}_{uj}$, respectively, the distance (d) between both vectors provides a measure of the two systems' mathematical similarity (see Figure 2b). The distance can be calculated according to

$$d = \sqrt{(e_{ui} - e_{uj})^2 + (s_{ui} - s_{uj})^2 + (a_{ui} - a_{uj})^2 + (b_{ui} - b_{uj})^2 + (\upsilon_{ui} - \upsilon_{uj})^2} \tag{8}$$

where all the coefficients have been normalized. The smaller the distance value is, the more mathematically similar are the two compared systems. For instance, if two i and j LFERs are linearly related, they will show the same normalized vector:

$$\log \mathrm{SP}_i = c_i + l_i\vec{w}_u \tag{9}$$

$$\log \mathrm{SP}_j = c_j + l_j\vec{w}_u \tag{10}$$

The d distance will be zero, and it is obvious that each LFER system may model the other, although the D' parameter is not zero in this situation, since

$$D' = l_j - l_i \tag{11}$$

On the other hand, we can relate the d distance parameter with the Ishihama cos θ_{ij} by simple trigonometry, since the two

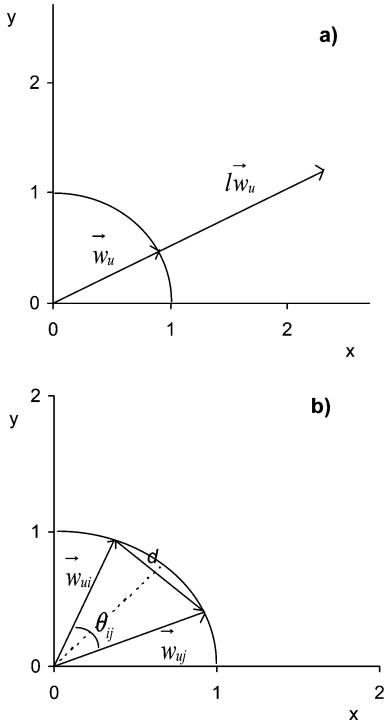

Figure 2. Schematic representation in two dimensions of a LSER vector normalization (a) and the distance d between two normalized vectors (b).

unitary vectors and the distance (d) constitute an isosceles triangle. This relation can be written as follows:

$$\cos \theta_{ij} = \cos(2 \arcsin(d/2)) \qquad (12)$$

This equation shows that both parameters measure the same concept. The $\cos \theta_{ij}$ is a measure of similarity (the higher the $\cos \theta_{ij}$ is, the larger the similarity of the systems is), and d is a measure of distance (the lower d is, the closer the two systems are). When the two systems approach each other, d tends to 0 and $\cos \theta_{ij}$ to 1.

Experimental Section

Apparatus. The retention data were measured in an IAM.PC.DD2 column (100 mm × 4.6 mm i.d., 12 μm, Regis Technologies Inc., Morton Grove, IL) and XTerra MSC18 and XTerra RP18 columns (150 mm × 4.6 mm i.d., 5 μm, Waters Corporation, Milford, MA). All measurements were performed with a Shimadzu liquid chromatograph (Kyoto, Japan) equipped with two Shimadzu LC-10AD pumps and a Shimadzu SPD-10AV detector. The temperature was controlled at 25.0 ± 0.1 °C with a Shimadzu CTO-10AS column oven. All pH measurements were taken with a Ross combination electrode Orion 8102 (glass electrode and a reference electrode with a 3.0 M KCl solution in water as salt bridge) in a Crison micro-pH 2002 potentiometer with a precision of ±0.1 mV (±0.002 pH units).

Chemicals. Acetonitrile was HPLC grade from Merck (Darmstadt, Germany) and water purified by the Milli-Q plus system from Millipore, with a resistivity of 18.2 MΩ cm. The sodium dihydrogenphosphate monohydrate (GR), the disodium hydrogenphosphate (GR), and the sodium hydroxide (GR) were from Merck. The test solutes employed were reagent grade or better and obtained from Merck, Fluka (Steinheim, Germany), Aldrich (Steinheim, Germany), or Carlo Erba (Milano, Italy).

Procedure. The eluents were mixtures of acetonitrile and 0.01 M phosphate aqueous buffer adjusted to pH 7, in percentages ranging from 10% to 60% for the IAM.PC.DD2 column and from 20% to 60% for the XTerra columns because of the extremely large retention times of several solutes in these columns. All compounds were dissolved in methanol, and their concentrations were 0.1 mg mL^{-1}. The injection volume was always 10 μL. The detection wavelength was 254 nm for all the compounds (except geraniol, α-pinene, pyrrole, furan, 4-hydroxybenzyl alcohol, lidocain, and *p*-cresole, whose wavelength was at 214 nm). Isocratic conditions were always used at a flow rate of 1 mL min^{-1}. The column holdup time was determined by using an aqueous solution of potassium bromide (0.1 mg mL^{-1}) as an unretained solute. Its detection was performed at 200 nm. Retention data were expressed by the logarithm of the capacity factor, log k, defined as $\log k = \log[(t_r - t_o)/t_o]$ where t_r and t_o are the retention times of the solute and the unretained compound, respectively. All measurements were taken in triplicate.

Results and Discussion

Characterization of Chromatographic Systems. IAM.PC.DD2, XTerra MSC18, and XTerra RP18 columns have been characterized with the solvation parameter model through eq 1 by analysis of the log k data of 59 solutes. This set of solutes with known descriptors must have properties sufficiently varied to define properly all interactions in eq 1. In a previous study[28] we selected an adequate collection of 71 solutes from the current database, which contains 2975 solutes with all five descriptors characterized. We applied principal component analysis (PCA) in order to select compounds that embraced a wide range of descriptor values, avoiding cross-correlation among the descriptors. In this study we have used 59 of these solutes that have a reasonable absorbance for their detection and are neutral at the working pH. We must emphasize again that characterization by the solvent parameter model requires a set of solutes neutral at the working pH with well-known descriptors. Thus, the solutes selected are neutral at pH 7; they are mostly monofunctional and only part of them are druglike molecules because descriptors for most drugs and complex structures are not yet available. The conclusions of this study might not be applicable to molecules with a more complex structure and surely not to ionized or partly ionized solutes.

The solute descriptors and the log k values obtained in the different chromatographic systems are given in Table 1 except for some compounds that could not be measured in all mobile phases because of their strong retention. The structures and properties of these columns have been given before.[35] The structure of the IAM.PC.DD2 column shows positive and negative charges in the IAM surface, but we consider that they do not affect significantly the distribution of neutral solutes through the stationary phase.

The system constants and the statistics for the fit of the solvation parameter model to the experimental log k data are summarized in Table 2. The outliers (solutes with a standard residual greater than |2.5|) were removed when the models were calculated (two to six outliers for correlation). Table 2 shows that the solvation parameter model gives good statistical fits and correlation coefficients. As far as we know, there are only two studies in the literature[30,31] reporting LSER parameters for IAM columns. Both refer to 20% acetonitrile, but there are some differences in the coefficients obtained by both sets of authors. Our coefficients for 20% acetonitrile in Table 2 are between those reported in these previous studies. Our e and v are very similar to those reported by Lepont and Poole,[31] while the a and b are closer to the coefficients established by Valko et al.[30] The s coefficient shows small differences with both literature values. Regarding XTerra columns, there are not LSER correlations reported, but we have compared the coefficient ratios (e/v, s/v, a/v, b/v) with those reported in a previous study[29] for different C18 columns with acetonitrile−water mobile phases, and they are in good agreement.

Table 1. Solute Descriptors and Retention Factors (log *k*) of All Studied Solutes

	descriptors					IAM.PC.DD2, ϕ_{ACN}[a]				XTerra MSC18, ϕ_{ACN}[a]			XTerra RP18, ϕ_{ACN}[a]		
solute	*E*	*S*	*A*	*B*	*V*	0.6	0.4	0.2	0.1	0.6	0.4	0.2	0.6	0.4	0.2
2,3-benzofuran	0.888	0.83	0.00	0.15	0.9053	−0.498	−0.404	0.879	1.194	0.305	0.870	1.683	0.242	0.805	1.525
2,3-dimethylphenol	0.850	0.90	0.52	0.36	1.0569	−0.432	0.095	0.799	1.152	0.037	0.521	1.301	0.084	0.570	1.250
2,4-dimethylphenol	0.840	0.80	0.53	0.39	1.0569	−0.441	0.096	0.804	1.170	0.027	0.535	1.326	0.085	0.574	1.265
2-naphthol	1.520	1.08	0.61	0.40	1.1441	−0.318	0.260	1.130	1.614	0.013	0.548	1.418	0.105	0.646	1.493
2-nitroaniline	1.180	1.37	0.30	0.36	0.9904	−0.586	−0.076	0.554	0.847	−0.060	0.363	1.021	−0.008	0.430	1.003
2-nitroanisole	0.968	1.34	0.00	0.38	1.0902	−0.701	−0.154	0.486	0.799	0.035	0.519	1.220	0.015	0.495	1.098
3-chloroaniline	1.050	1.10	0.30	0.36	0.9390	−0.547	−0.023	0.636	0.911	0.016	0.467	1.144	0.036	0.495	1.085
3-nitroaniline	1.200	1.71	0.40	0.35	0.9904	−0.642	−0.155	0.408	0.664	−0.153	0.286	0.852	−0.073	0.346	0.858
4-chloroacetanilide	0.980	1.50	0.64	0.51	1.2357	−0.538	−0.074	0.626	1.009	−0.187	0.243	1.040	−0.109	0.310	1.033
4-chloroaniline	1.060	1.10	0.30	0.35	0.9390	−0.552	−0.050	0.589	0.878	−0.022	0.410	1.084	−0.009	0.426	1.010
4-chlorophenol	0.915	1.08	0.67	0.20	0.8975	−0.371	0.153	0.884	1.249	−0.056	0.418	1.210	0.038	0.518	1.215
4-nitroaniline	1.220	1.91	0.42	0.38	0.9904	−0.604	−0.149	0.461	0.760	−0.211	0.170	0.751	−0.119	0.293	0.825
acetanilide	0.870	1.36	0.46	0.69	1.1137	−0.759	−0.402	0.042	0.298	−0.364	−0.109	0.429	−0.325	−0.041	0.422
acetophenone	0.818	1.01	0.00	0.48	1.0139	−0.747	−0.283	0.247	0.522	−0.029	0.360	0.976	−0.064	0.316	0.828
α-pinene	0.446	0.14	0.00	0.12	1.2574	0.034	0.289			1.262			0.938		
aniline	0.955	0.96	0.26	0.50	0.8162	−0.744	−0.368	0.003	0.155	−0.229	0.071	1.207	−0.213	0.070	0.379
anisole	0.708	0.75	0.00	0.29	0.9160	−0.627	−0.085	0.516	0.771	0.194	0.687	1.353	0.126	0.601	1.159
antipyrine	1.320	1.50	0.00	1.48	1.5502	−0.833	−0.565	−0.182	0.092	−0.571	−0.367	0.239	−0.551	−0.381	0.110
benzaldehyde	0.820	1.00	0.00	0.39	0.8730	−0.713	−0.286	0.189	0.404	−0.053	0.338	0.869	−0.065	0.302	0.747
benzamide	0.990	1.50	0.49	0.67	0.9728	−0.807	−0.555	−0.220	−0.005	−0.582	−0.403	−0.197	−0.537	−0.347	0.025
benzene	0.610	0.52	0.00	0.14	0.7164	−0.580	−0.061	0.493	0.663	0.262	0.735	1.324	0.164	0.631	1.132
benzophenone	1.447	1.50	0.00	0.50	1.4808	−0.448	0.236	1.196	1.683	0.382	1.065	2.104	0.333	0.974	1.929
benzonitrile	0.742	1.11	0.00	0.33	0.8711	−0.715	−0.236	0.287	0.512	0.004	0.425	1.004	−0.020	0.393	0.881
benzyl benzoate	1.264	1.42	0.00	0.51	1.6804	−0.375	0.452	1.655	2.232	0.620	1.435		0.509	1.304	
bromobenzene	0.882	0.73	0.00	0.09	0.8914	−0.363	0.267	1.067	1.389	0.456	1.069	1.896	0.368	0.956	1.729
butylbenzene	0.600	0.51	0.00	0.15	1.2800	−0.179	0.653	1.835		0.953	1.798		0.720	1.543	
butyrophenone	0.797	0.95	0.00	0.51	1.2957	−0.556	0.066	0.829	1.237	0.348	0.932	1.808	0.257	0.824	1.612
caffeine	1.500	1.60	0.00	1.33	1.3632	−0.894	−0.734	−0.506	−0.210	−0.599	−0.560	−0.199	−0.575	−0.479	−0.221
chlorobenzene	0.718	0.65	0.00	0.07	0.8388	−0.430	0.191	0.945	1.231	0.408	0.999	1.766	0.321	0.888	1.615
corticosterone	1.860	3.43	0.40	1.63	2.7389	−0.543	−0.081	0.819	1.444	−0.174	0.284	0.780	−0.202	0.251	1.406
cortisone	1.960	3.50	0.36	1.87	2.7546	−0.736	−0.310	0.487	1.076	−0.388	0.010	1.225	−0.367	0.038	1.079
dodecanophenone	0.720	0.95	0.00	0.50	2.4229	0.382	1.637			1.873			1.484		
estradiol	1.800	3.30	0.88	0.95	2.1988	0.014	0.639	1.836		−0.004	0.604		0.181	0.807	
estriol	2.000	3.36	1.40	1.22	2.2575	−0.289	0.109	1.059	1.328	−0.560	−0.183	0.897	−0.385	0.054	1.188
ethylbenzene	0.613	0.51	0.00	0.15	0.9982	−0.404	0.276	1.104	1.419	0.587	1.239	2.116	0.425	1.068	1.852
furan	0.369	0.53	0.00	0.13	0.5363	−0.735	−0.358	0.025	0.104	0.001	0.356	0.732	−0.048	0.304	0.601
geraniol	0.513	0.63	0.39	0.66	1.4903	−0.451	−0.067	1.050	1.464	0.260	0.861	1.980	0.153	0.742	1.730
heptanophenone	0.720	0.95	0.00	0.50	1.7184	−0.227	0.642	1.909	2.477	0.898	1.775		0.709	1.561	
hydrocortisone	2.030	3.49	0.71	1.90	2.7975	−0.590	−0.232	0.540	1.112	−0.410	−0.043	0.944	−0.374	0.000	1.055
m-cresole	0.822	0.88	0.57	0.34	0.9160	−0.527	−0.077	0.505	0.810	−0.122	0.279	0.940	−0.067	0.343	0.895
methyl benzoate	0.733	0.85	0.00	0.46	1.0726	−0.648	−0.116	0.521	0.819	0.151	0.622	1.368	0.086	0.549	1.177
monuron	1.140	1.50	0.47	0.78	1.4768	−0.605	−0.115	0.574	0.979	−0.181	0.257	1.050	−0.121	0.306	1.024
myrcene	0.483	0.29	0.00	0.21	1.0000	−0.147	0.745	2.001		1.082			0.804		
naphthalene	1.340	0.92	0.00	0.20	1.0854	−0.299	0.390	1.323	1.762	0.533	1.202	2.171	0.436	1.089	1.995
nitrobenzene	0.871	1.11	0.00	0.28	0.8906	−0.636	−0.090	0.503	0.747	0.107	0.584	1.220	0.077	0.549	1.087
o-toluidine	0.970	0.90	0.23	0.59	0.9571	−0.672	−0.255	0.211	0.424	−0.100	0.267	0.463	−0.104	0.243	0.667
phenol	0.805	0.89	0.60	0.30	0.7751	−0.617	−0.223	0.250	0.476	−0.238	0.083	0.583	−0.173	0.164	0.586
propiophenone	0.804	0.95	0.00	0.51	1.1548	−0.642	−0.099	0.544	0.878	0.179	0.666	1.500	0.112	0.591	1.227
propylbenzene	0.604	0.50	0.00	0.15	1.1391	−0.294	0.472	1.458	1.845	0.769	1.520		0.571	1.306	
p-xylene	0.613	0.52	0.00	0.16	0.9982	−0.380	0.293	1.121	1.455	0.584	1.248	2.129	0.436	1.075	1.854
pyrimidine	0.606	1.00	0.00	0.65	0.6342	−0.854	−0.735	−0.637	−0.544	−0.606	−0.604	−0.534	−0.590	−0.517	−0.516
pyrocatechol	0.970	1.10	0.88	0.47	0.8338	−0.555	−0.248	0.124	0.329	−0.447	−0.238	0.170	−0.380	−0.137	0.194
pyrrole	0.613	0.73	0.41	0.29	0.5774	−0.748	−0.397	−0.096	−0.007	−0.216	0.052	0.321	−0.200	0.078	0.284
quinoline	1.268	0.97	0.00	0.51	1.0443	−0.451	0.237	1.196	1.685	−0.107	0.224	1.174	−0.165	0.167	0.778
resorcinol	0.980	1.00	1.10	0.58	0.8338	−0.653	−0.376	0.000	0.249	−0.569	−0.380	−0.022	−0.491	−0.260	0.073
thiourea	0.840	0.82	0.77	0.87	0.5696	−0.803	−0.732	−0.687	−0.641	−0.953	−1.166	−1.158	−0.966	−1.047	−1.264
thymol	0.822	0.79	0.52	0.44	1.3387	−0.309	0.385	1.356	1.795	0.352	1.034	2.080	0.352	1.020	1.959
toluene	0.601	0.52	0.00	0.14	0.8573	−0.480	0.116	0.809	1.066	0.412	0.988	1.707	0.298	0.847	1.517
valerophenone	0.795	0.95	0.00	0.50	1.4366	−0.456	0.246	1.190	1.611	0.513	1.209	2.232	0.405	1.065	2.000

[a] ϕ_{ACN} represents the different volume fractions of acetonitrile in the three studied columns.

Table 2. Constants for All Studied Chromatographic Systems (Standard Deviations in Parentheses)

	coefficients						statistics			
system	*c*	*e*	*s*	*a*	*b*	*v*	*n*	*r*	SD	*F*
IAM.PC.DD2 (10% acetonitrile)	−0.730(0.039)	0.761(0.059)	−0.774(0.042)	0.128(0.035)	−1.963(0.050)	2.400(0.045)	49	0.994	0.068	708
IAM.PC.DD2 (20% acetonitrile)	−0.705(0.038)	0.498(0.058)	−0.577(0.042)	0.187(0.034)	−1.999(0.057)	2.131(0.038)	52	0.994	0.066	742
IAM.PC.DD2 (40% acetonitrile)	−0.710(0.027)	0.292(0.042)	−0.344(0.029)	0.141(0.024)	−1.193(0.040)	1.161(0.027)	51	0.991	0.047	480
IAM.PC.DD2 (60% acetonitrile)	−0.978(0.028)	0.268(0.041)	−0.258(0.028)	0.189(0.025)	−0.593(0.035)	0.616(0.028)	55	0.963	0.050	125
XTerra MSC18 (20% acetonitrile)	−0.149(0.049)	0.272(0.076)	−0.669(0.053)	−0.432(0.045)	−2.346(0.060)	2.764(0.062)	49	0.993	0.093	606
XTerra MSC18 (40% acetonitrile)	−0.152(0.036)	0.151(0.059)	−0.463(0.038)	−0.424(0.034)	−1.719(0.043)	1.759(0.039)	55	0.994	0.072	764
XTerra MSC18 (60% acetonitrile)	−0.295(0.034)	−0.003(0.054)	−0.333(0.035)	−0.317(0.033)	−1.108(0.041)	1.191(0.030)	58	0.991	0.069	551
XTerra RP18 (20% acetonitrile)	−0.281(0.032)	0.375(0.052)	−0.579(0.038)	−0.211(0.030)	−2.352(0.046)	2.564(0.040)	48	0.996	0.060	1189
XTerra RP18 (40% acetonitrile)	−0.172(0.029)	0.233(0.047)	−0.460(0.032)	−0.260(0.027)	−1.574(0.036)	1.582(0.028)	55	0.996	0.056	1121
XTerra RP18 (60% acetonitrile)	−0.330(0.020)	0.120(0.034)	−0.335(0.023)	−0.195(0.020)	−0.996(0.026)	1.025(0.018)	55	0.996	0.040	1229

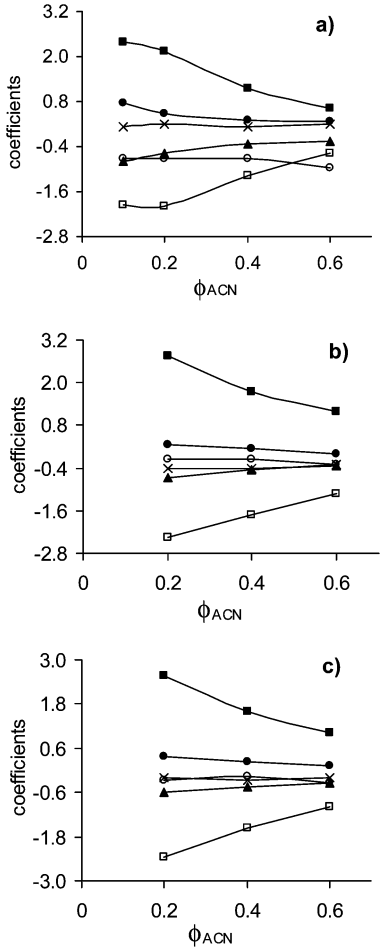

Figure 3. Plot of LSER coefficients vs volume fraction of acetonitrile in the mobile phase, using as stationary phase a IAM.PC.DD2 (a), a XTerra MSC18 (b), and a XTerra RP18 (c) columns: (■) coefficient *v*; (●) coefficient *e*; (×) coefficient *a*; (▲) coefficient *s*; (□) coefficient *b*; (○) constant *c*.

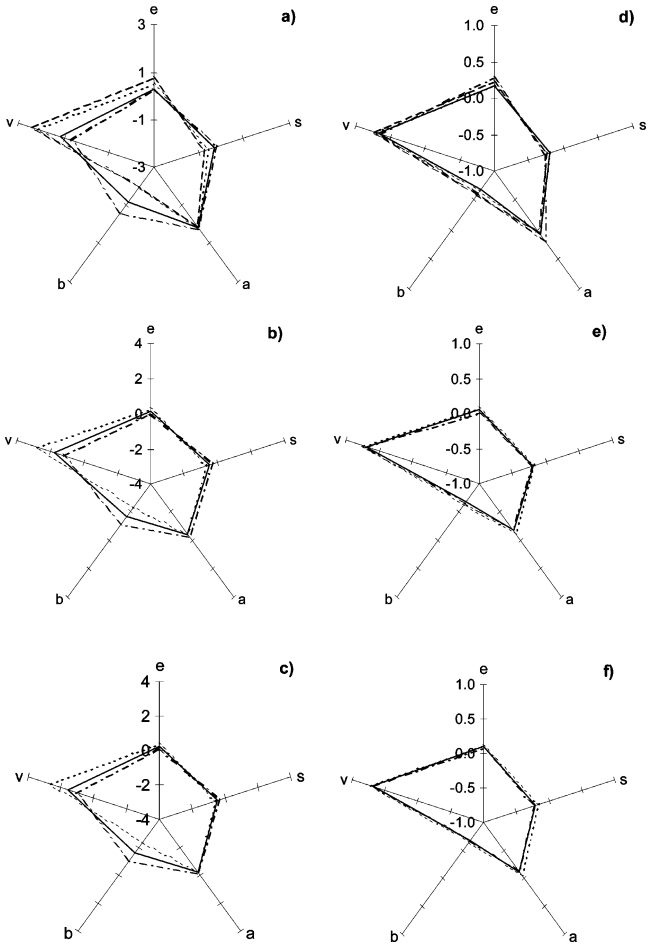

Figure 4. Radial plots of LSER coefficients before and after their normalization, in IAM.PC.DD2 column ((a) and (d), respectively), in XTerra MSC18 ((b) and (e), respectively), and in XTerra RP18 ((c) and (f), respectively): (- · -) $\phi_{ACN} = 0.6$; (−) $\phi_{ACN} = 0.4$; (···) $\phi_{ACN} = 0.2$; (- - -) $\phi_{ACN} = 0.1$.

Positive coefficients imply an increase in log *k*; i.e., partition into the stationary phase is favored. Therefore, negative coefficients indicate a greater affinity to the mobile phase. The larger the coefficient absolute value, the greater the influence on the retention in RPLC. The comparison between the coefficients of each system shows that solute volume and hydrogen-bond acidity are the largest coefficients in absolute value (*v* and *b*, respectively). The coefficient *v* is large and positive in all cases, and its value increases with the water content in the mobile phase. This is due to the cohesive density of water. Therefore, creating a cavity inside the mobile phase requires more energy than is necessary in the stationary phase. All coefficients *b* are large and negative, which indicates that the hydrogen-bond acidity of the stationary phase is lower than the hydrogen-bond acidity of the mobile phase. Thus, solutes with greater hydrogen-bond basicity (large *B* descriptor value) are less retained.

All systems have negative *s* coefficient values, which shows that stationary phases are less dipolar than mobile phases. Regarding the coefficient *e*, all systems have positive values, which indicates that stationary phases are more polarizable than mobile phases.

The *aA* term depends on the column. Both XTerra columns have negative *a* coefficient values; therefore, the stationary phase has a lower hydrogen-bond basicity than the mobile phase. However, the IAM.PC.DD2 column has a positive coefficient *a*, which indicates that this stationary phase is a stronger hydrogen-bond base than is the mobile phase. Thus, IAM has stronger affinity to hydrogen-bond donor compounds than C18 columns. This is the main difference between all the columns.

The different proportions of the acetonitrile−water mobile phases change the properties of the mobile phase and therefore the values of the coefficients (see Table 2 and Figure 3). For the IAM column the hydrogen-bond acidity of the mobile phase, with respect to the same property of the solvated stationary phase, is reduced significantly by addition of acetonitrile (coefficient *b* increases). However, the lipophilicity of the mobile phase is significantly increased by the addition of acetonitrile (coefficient *v* decreases); i.e., the cohesion of the mobile phase is strongly reduced when the content of acetonitrile in the mobile phase increases. These properties change little at first (10−20%) and more noticeably from 20% to 60% of organic modifier. The variation of the other properties is smaller, but there is a moderate increase in the polarizability (coefficient *e* decreases) and a decrease in the dipolarity (coefficient *s* increases) of the mobile phase with acetonitrile content. However, the hydrogen-bond basicity of the system is hardly influenced by the composition of the mobile phase. Therefore, solutes that differ in size and hydrogen-bond basicity will show the greatest change in retention with increasing acetonitrile content of the mobile phase. The same trends are observed in all the studied stationary phases.

Modeling of Biological Processes. The LFER coefficients of selected biological systems were obtained from the literature and are summarized in Table 3.

Table 3. Constants for All Selected Biopartitioning Systems

		coefficients						statistics			
number	biopartitioning systems	*c*	*e*	*s*	*a*	*b*	*v*	*n*	*r*	SD	*F*
1	blood−brain distribution[19]	0.044	0.511	−0.886	−0.724	−0.666	0.861	148	0.843	0.367	71
2	blood−brain permeability[18]	−1.210	0.770	−1.870	0.000	−2.800	3.310	18	0.976	0.481	65
3	human intestinal absorption[22]	0.544	−0.025	0.141	−0.409	−0.514	0.204	127	0.894	0.290	94
4	human skin permeation[17]	−5.426	−0.106	−0.473	−0.473	−3.000	2.296	119	0.912	0.461	112
5	human skin partition[17]	0.341	0.341	−0.206	−0.024	−2.178	1.850	45	0.962	0.216	97
6	tadpole narcosis[16]	0.582	0.770	−0.696	0.243	−2.592	3.343	114	0.952	0.341	263
7	octanol−water distribution[15]	0.088	0.562	−1.054	0.034	−3.460	3.814	613	0.997	0.116	23 162
	tissue−blood partition										
8	brain[23]	0.523	0.195	−0.603	−0.627	−0.623	0.627	302	0.75	0.30	138
9	muscle[24]	0.039	−0.100	−0.080	−0.254	0.041	0.233	163	0.595	0.220	33

Table 4. Distances (d, D') and cos θ_{ij} Obtained between All Studied Chromatographic Columns with 40% of Acetonitrile and Selected Biopartitioning Systems

	chromatographic systems, 40% of acetonitrile								
	IAM.PC.DD2			XTerra MSC18			XTerra RP18		
biopartitioning systems	d	D'	cos θ_{ij}	d	D'	cos θ_{ij}	d	D'	cos θ_{ij}
blood−brain distribution	0.712	1.208	0.747	0.603	1.521	0.818	0.605	1.348	0.817
blood−brain permeability	0.234	3.127	0.973	0.300	2.473	0.955	0.250	2.614	0.969
human intestinal absorption	0.888	1.420	0.606	0.702	2.065	0.754	0.747	1.863	0.721
human skin permeation	0.317	2.260	0.950	0.181	1.413	0.984	0.200	1.644	0.980
human skin partition	0.179	1.222	0.984	0.223	0.694	0.975	0.187	0.754	0.983
tadpole narcosis	0.143	2.661	0.990	0.276	2.038	0.962	0.223	2.176	0.975
octanol−water distribution	0.116	3.573	0.993	0.184	2.825	0.983	0.128	3.014	0.992
tissue−blood partition									
brain	0.696	1.130	0.758	0.527	1.595	0.861	0.549	1.405	0.850
muscle	1.194	1.663	0.2871	1.001	2.380	0.499	1.049	2.164	0.450

Table 5. Distances (d) Obtained between All Selected Biopartitioning Systems

biopartitioning systems		1	2	3	4	5	6	7	8	9
blood−brain distribution	1	0								
blood−brain permeability	2	0.544	0							
human intestinal absorption	3	0.917	0.954	0						
human skin permeation	4	0.728	0.412	0.643	0					
human skin partition	5	0.757	0.368	0.742	0.199	0				
tadpole narcosis	6	0.706	0.250	0.909	0.372	0.238	0			
octanol−water distribution	7	0.674	0.213	0.848	0.268	0.182	0.121	0		
tissue−blood partition										
brain	8	0.199	0.550	0.779	0.627	0.705	0.702	0.642	0	
muscle	9	0.879	1.085	1.032	1.087	1.175	1.127	1.103	0.819	0

Estimation of the Similarity between Systems. To compare chromatographic and biological systems, we propose to use the distance (d) between these systems calculated according to eq 8, where all the coefficients are normalized. When all components of the system vectors are represented (see Figure 4a−c), we can observe large differences depending on the mobile phase composition. However, if the system coefficients are normalized (see Figure 4d−f), these differences practically disappear, and the distances between them become very small. There are significant differences in the retention of the solutes depending on the concentration of acetonitrile, so we obtain very different coefficients for each mobile phase composition (see Figure 3). However, the differences between these chromatographic systems are minimized when we normalize the coefficients. If we calculate the distance d between systems with the same stationary phase and extreme percentages of acetonitrile (IAM.PC.DD2 $d = 0.192$ from 10% to 60% acetonitrile; XTerra MSC18 $d = 0.114$ from 20% to 60% acetonitrile; XTerra RP18 $d = 0.104$ from 20% to 60% acetonitrile), we can conclude that these systems are analogous. For this reason, it is not necessary to calculate d between all chromatographic and biological systems. We choose 40% of acetonitrile as an intermediate and representative mobile phase composition, and estimate d between all columns with this percentage and all biological systems. The results are shown in Table 4. The distance D', where the system coefficients are not normalized, and cos θ_{ij}, calculated according to eq 2, are also presented in this table. Obviously, the same conclusions about the similarity of the systems will be obtained if we use d or cos θ_{ij}, since they are related by a trigonometric equation. If cos θ_{ij} is near 1, the distance d is short (0−0.25), and the two compared systems can be considered similar. However, we consider it to be easier and more intuitive to compare partition systems by means of the d parameter, since the cos θ_{ij} scale is not linear. Both d and cos θ_{ij} scales range from 0 to 1, but because of the lack of linearty in the cos θ_{ij} scale, the range of the adequate cosines for similar systems goes from 1 to 0.97 while the distances go from 0 to 0.25. The wider and linear range allows us to observe at first sight the small differences between various systems, which is more difficult with the cosine range. On the other hand, D' does not provide the same information, as was proved by eq 11, since it is possible that two systems are separated by a small d but a large D' distance. For example, the distances D' for the chromatographic systems studied above are very large (IAM.PC.DD2 $D' = 2.360$ between 10% and 60% acetonitrile; XTerra MSC18 $D' = 2.052$ between 20% and 60% acetonitrile; XTerra RP18 $D' = 2.081$ between 20% and 60% acetonitrile). It is obvious that these long distances point to poor similarity of related systems for which d indicates close similarity (e.g., $D' = 2.081$ but $d = 0.104$ between 20% and

Table 6. Solute Descriptors and Retention Factors (log *k*) of Some Selected Solutes from ref 17 in the Three Studied Columns

	descriptors					log *k*, $\phi_{ACN} = 0.4$		
solute	*E*	*S*	*A*	*B*	*V*	IAM.PC.DD2	XTerra MSC18	XTerra RP18
2,4,6-trichlorophenol	1.010	0.80	0.68	0.15	1.1423	−0.229	0.228	0.281
2,4-dichlorophenol	0.960	0.84	0.53	0.19	1.0199	0.376	0.651	0.767
2-chlorophenol	0.853	0.88	0.32	0.31	0.8975	1.014	0.326	0.429
2-nitro-*p*-phenylendiamine	1.525	2.05	0.35	0.70	1.0902	−0.412	−0.237	−0.126
3-nitrophenol	1.050	1.57	0.79	0.23	0.9493	−0.011	0.214	0.381
4-amino-2-nitrophenol	1.360	1.50	0.30	0.66	1.0491	−0.331	0.005	0.082
4-bromophenol	1.080	1.17	0.67	0.20	0.9501	0.187	0.463	0.583
4-chloro-3-methylphenol	0.920	1.02	0.67	0.22	1.0384	0.250	0.587	0.683
4-hydroxybenzyl alcohol	0.998	1.20	0.86	0.81	0.9747	−0.544	−0.516	−0.457
4-nitrophenol	1.070	1.72	0.82	0.26	0.9493	−0.262	−0.070	0.114
8-methoxypsoralen	1.611	1.70	0.00	0.80	1.4504	−0.068	0.451	0.477
cortisone 21-acetate	1.820	3.11	0.21	2.13	3.0521	−0.088	0.573	0.593
hydrocortisone 21-acetate	1.890	2.88	0.46	2.16	3.0951	−0.066	0.470	0.525
lidocaine	1.010	1.49	0.11	1.27	2.0589	0.349	0.753	0.613
o-phenylenediamine	1.260	1.40	0.24	0.73	0.9160	−0.507	−0.390	−0.354
p-cresole	0.820	0.87	0.57	0.31	0.9160	−0.093	0.261	0.334
progesterone	1.450	3.29	0.00	1.14	2.6215	0.425	1.287	1.122
testosterone	1.540	2.59	0.32	1.19	2.3827	0.232	0.630	0.611

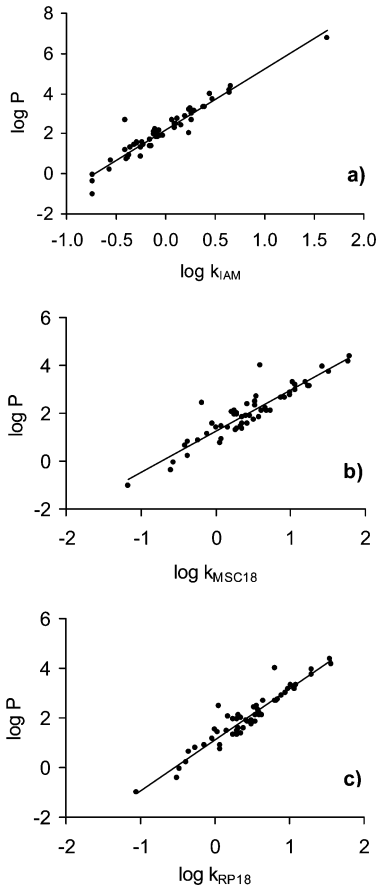

Figure 5. Plots of experimental log *P* vs experimental log *k* in IAM.PC.DD2 (a), XTerra MSC18 (b), and XTerra RP18 (c) columns.

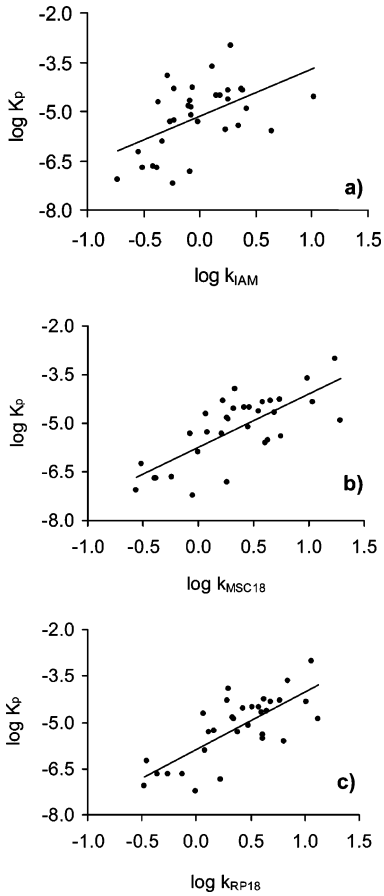

Figure 6. Plots of experimental log K_p (skin permeation logarithm) vs experimental log *k* (retention factor logarithm) in IAM.PC.DD2 (a), XTerra MSC18 (b), and XTerra RP18 (c) columns.

60% acetonitrile in XTerra RP18). This fact can be also observed when we compare biological with chromatographic systems (Table 4). There is a short D' distance (1.208) between blood−brain distribution and IAM.PC.DD2 but a large *d* distance (0.712). In contrast, the D' distance between IAM.PC.DD2 and blood−brain permeability is large (3.127) but *d* is short (0.234).

If the values of *d* are analyzed, blood−brain permeability, human skin partition, tadpole narcosis, and octanol−water distribution would be the only systems considered as analogues to the IAM.PC.DD2 with 40% of acetonitrile system ($d < 0.25$), while the human skin permeation would be better explained by means of the XTerra MSC18 ($d = 0.18$). However, the small differences between the XTerra RP18 and IAM.PC.DD2 columns in relation to the *d* parameter suggest that the XTerra RP18 column could provide good correlations with the same biological systems as well (see Table 4). On the other hand, according to D', the XTerra columns should be good models for the human skin partition ($D' < 0.8$). Finally, some biological systems, such as the blood−brain distribution and the tissue−blood partition (for muscle), cannot be modeled with any of these chromatographic systems because all values of the distance parameter are too large.

We can also compare all biological systems between them by means of the *d* parameter (see Table 5). Not surprisingly, blood−brain distribution and the tissue−blood partition (for brain) are similar systems, and the same similarity can be found between human skin permeation and partition. Regarding the other systems, tadpole narcosis and octanol−water distribution are analogue to blood−brain permeability and human skin partition. Moreover, octanol−water distribution is also similar to tadpole narcosis. The rest of the systems are too different between them, according to *d*.

Examples of Modeling. According to *d*, the octanol−water distribution should be well modeled by means of IAM.PC.DD2 ($d = 0.12$) and XTerra RP18 ($d = 0.13$) and slightly worse by XTerra MSC18 ($d = 0.18$), although taking into account D', they cannot be considered similar systems because the distances are very large. Thus, according to the *d* distance, a good linear relationship should be obtained between the logarithm of the retention factor ($\log k$) and the logarithm of octanol−water partition coefficient ($\log P$). The $\log P$ data for all studied solutes were obtained from refs 15, 36, 37 (except α-pinene, geraniol, and myrcene, which were not available), and their plots against $\log k$ are presented in Figure 5. Three correlations were obtained (for IAM.PC.DD2, XTerra MSC18, and XTerra RP18 columns, respectively):

$$\log P = 2.185 + 3.034 \log k_{IAM} \quad (13)$$
$$n = 56, \quad r = 0.960, \quad SD = 0.362$$

$$\log P = 1.231 + 1.722 \log k_{MSC18} \quad (14)$$
$$n = 55, \quad r = 0.924, \quad SD = 0.433$$

$$\log P = 1.109 + 2.040 \log k_{RP18} \quad (15)$$
$$n = 55, \quad r = 0.952, \quad SD = 0.347$$

In these equations and in the following ones, *n* denotes the number of solutes, *r* is the correlation coefficient, and SD is the standard deviation. It is obvious that there are good correlations in all cases, specially for IAM.PC.DD2 and XTerra RP18, since they present better statistics as is predicted by our *d* distance. The correlations embrace a large large lipophilicity range of 7 $\log P$ units, with very few outliers (2,3-benzofuran and thiourea for IAM.PC.DD2; estradiol and estriol for XTerra MSC18 and XTerra RP18). These results are in good agreement with other ones published before,[38−42] where it was shown that HPLC can be used to determine $\log P$ easily using suitable stationary and mobile phases.

The human skin permeation and partition systems were also selected in order to be modeled by chromatographic systems. The experimental data of $\log K_p$ (skin permeation) and $\log K_{sc}$ (skin partition) were extracted from ref 17. Seventeen substances from Table 1 (2-naphthol, 4-chlorophenol, aniline, anisole, benzaldehyde, benzene, caffeine, corticosterone, cortisone, estradiol, ethylbenzene, hydrocortisone, *m*-cresole, phenol, resorcinol, thymol, and toluene) were included in this study, since their experimental $\log K_p$ or $\log K_{sc}$ values were known. Moreover, a set of new solutes was selected and studied in the three columns, using 40% of acetonitrile. Their descriptors and the experimental $\log k$ data are summarized in Table 6.

Plots of experimental $\log K_p$ versus experimental $\log k$ for the selected solutes in the three columns are shown in Figure 6. Three correlations were obtained (for IAM.PC.DD2, XTerra MSC18, and XTerra RP18 columns, respectively):

$$\log K_p = -5.154 + 1.443 \log k_{IAM} \quad (16)$$
$$n = 32, \quad r = 0.514, \quad SD = 0.916$$

$$\log K_p = -5.728 + 1.636 \log k_{MSC18} \quad (17)$$
$$n = 32, \quad r = 0.739, \quad SD = 0.719$$

$$\log K_p = -5.865 + 1.849 \log k_{RP18} \quad (18)$$
$$n = 32, \quad r = 0.746, \quad SD = 0.711$$

The human skin permeation gave fair correlations with XTerra MSC18 and XTerra RP18 (according to $d = 0.18$ and $d = 0.20$, respectively), while the IAM.PC.DD2 column ($d = 0.32$) showed such a poor correlation that it is not useful for predicting skin permeation. Although the *d* distance between XTerra and skin permeation is only slightly larger than the *d* distance between IAM (or XTerra) and octanol−water partition, the correlation is worse. This fact is due to the precision of the original data, since parameters for physicochemical processes (octanol−water distribution) can be measured more easily, precisely, and accurately than those for biological processes (skin permeation). This can be easily observed in the statistics (*r* and *F*) of the original LFER correlations presented in Table 3. Thus, there are two main factors that influence the precision (*r* and F) of the biological−chromatographic systems correlations. One is the similarity of the two systems correlated, measured by the *d* distance between them. The other one is the precision (e.g., standard deviation) with which the correlated data (both chromatographic and especially biological) have been measured. The larger the *d* distance among systems and the standard deviation of the biological data are, the poorer is the correlation with chromatographic parameters.

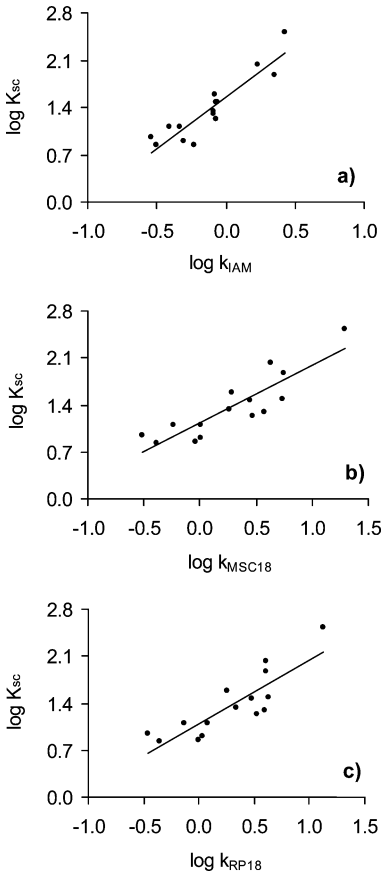

Figure 7. Plots of experimental $\log K_{sc}$ (skin partition logarithm) vs experimental $\log k$ (retention factor logarithm) in IAM.PC.DD2 (a), XTerra MSC18 (b), and XTerra RP18 (c) columns.

Good correlations were obtained between the human skin partition ($\log K_{sc}$) and chromatographic systems ($\log k$). Relationships are shown by the following:

$$\log K_{sc} = 1.555 + 1.522 \log k_{IAM} \quad (19)$$
$$n = 15, \quad r = 0.919, \quad SD = 0.196$$

$$\log K_{sc} = 1.131 + 0.855 \log k_{MSC18} \quad (20)$$
$$n = 15, \quad r = 0.872, \quad SD = 0.242$$

$$\log K_{sc} = 1.099 + 0.950 \log k_{RP18} \quad (21)$$
$$n = 15, \quad r = 0.847, \quad SD = 0.263$$

for IAM.PC.DD2, XTerra MSC18, and XTerra RP18 columns, respectively.

These correlations are illustrated in Figure 7. The best of them corresponds to the IAM.PC.DD2 column ($d = 0.179$), which has the smallest d. Statistics for the other two columns ($d = 0.223$ and 0.187) are not as good, although they are still quite reasonable.

Conclusions

It has been shown that the proposed d parameter is a good measure of the mathematical similarity between biological and chromatographic systems, previously characterized by means of the solvation parameter model. It allows a choice to be made for the most appropriate chromatographic system (IAM or C18) to model a particular biological system and to estimate drug distribution parameters in the biological system from retention measurements in the selected chromatographic column.

The results obtained demonstrate that contrary to common belief immobilized artificial membranes are not always the best choice to model a biological drug distribution system, since for some of them common C18 columns may show better performances. The octanol−water partition, tadpole narcosis, human skin partition, and blood−brain permeability can be well modeled by IAM columns, but human skin permeation is better modeled by C18 columns. Application of the d parameter shows that some biological systems (e.g., blood−brain or tissue−blood distribution) cannot be well modeled by IAM or C18 columns, and thus use of IAMs to estimate drug-distribution parameters for these systems is inadvisable.

Acknowledgment. We are grateful for financial support from the Spanish Government (Project CTQ2004-00965/BQU). E.L. was supported by Grant AP2002-3049 from the Spanish Government.

References

(1) Smith, R. N.; Hansch, C.; Ames, M. M. Selection of a reference partitioning system for drug design work. *J. Pharm. Sci.* **1975**, *64*, 599−606.
(2) Rogers, J. A.; Choi, Y. W. The liposome partitioning system for correlating biological activities of imidazolidine derivatives. *Pharm. Res.* **1993**, *10*, 913−917.
(3) Balon, K.; Riebesehl, B. U.; Müller, B. W. Drug liposome partitioning as a tool for the prediction of human passive intestinal absorption. *Pharm. Res.* **1999**, *16*, 882−888.
(4) Danelian, E.; Karlén, A.; Karlsson, R.; Winiwarter, S.; Hansson, A.; Löfas, S.; Lennernäs, H.; Hämäläinen, M. D. SPR biosensor studies of the direct interaction between 27 drugs and a liposome surface: correlation with fraction absorbed in humans. *J. Med. Chem.* **2000**, *43*, 2083−2086.
(5) Pidgeon, C.; Venkataram, U. V. Immobilized artificial membrane chromatography: supports composed of membrane lipids. *Anal. Biochem.* **1989**, *176*, 36−47.
(6) Pidgeon, C.; Ong, S.; Liu, H.; Qiu, X.; Pidgeon, M.; Dantzig, A. H.; Munroe, J.; Hornback, W. J.; Kasher, J. S.; Glunz, L.; Szczerba, T. IAM chromatography: an in vitro screen for predicting drug membrane permeability. *J. Med. Chem.* **1995**, *38*, 590−594.
(7) Nasal, A.; Sznitowska, M.; Bucinski, A.; Kaliszan, R. Hydrophobicity parameter from high-performance liquid chromatography on an immobilized artificial membrane column and its relationship to bioactivity. *J. Chromatogr. A* **1995**, *692*, 83−89.
(8) Barbato, F.; La Rotonda, M. I.; Quaglia, F. Chromatographic indexes on immobilized artificial membranes for local anesthetics: relationships with activity data on closed sodium channels. *Pharm. Res.* **1997**, *14*, 1699−1705.
(9) Salminen, T.; Pulli, A.; Taskinen, J. Relationship between immobilised artificial membrane chromatographic retention and the brain penetration of structurally diverse drugs. *J. Pharm. Biomed. Anal.* **1997**, *15*, 469−477.
(10) Reichel, A.; Begley, D. J. Potential of immobilized artificial membranes for predicting drug penetration across the blood−brain barrier. *Pharm. Res.* **1998**, *15*, 1270−1274.
(11) Genty, M.; González, G.; Clere, C.; Desangle-Gouty, V.; Legendre, J. Y. Determination of the passive absorption through the rat intestine using chromatographic indices and molar volume. *Eur. J. Pharm. Sci.* **2001**, *12*, 223−229.
(12) Valko, K.; Nunhuck, S.; Bevan, C.; Abraham, M. H.; Reynolds, D. P. Fast gradient HPLC method to determine compounds binding to human serum albumin. Relationships with octanol/water and immobilized artificial membrane lipophilicity. *J. Pharm. Sci.* **2003**, *92*, 2236−2248.
(13) Abraham, M. H. Scales of solute hydrogen-bonding: their construction and application to physicochemical and biochemical processes. *Chem. Soc. Rev.* **1993**, *22*, 73−83.
(14) Abraham, M. H.; Chadha, H. S.; Martins, F.; Mitchell, R. C.; Bradbury, M. W.; Gratton, J. A. Hydrogen bonding part 46: A review of the correlation and prediction of transport properties by an LFER method: physicochemical properties, brain penetration and skin permeability. *Pestic. Sci.* **1999**, *55*, 78−88.
(15) Abraham, M. H.; Chadha, H. S.; Whiting, G. S.; Mitchell, R. C. Hydrogen bonding. 32. An analysis of water−octanol and water−alkane partitioning and the $\Delta \log P$ parameter of seiler. *J. Pharm. Sci.* **1994**, *83*, 1085−1100.
(16) Abraham, M. H.; Ràfols, C. Factors that influence tadpole narcosis. An LFER analysis. *J. Chem. Soc., Perkin Trans. 2* **1995**, 1843−1851.
(17) Abraham, M. H.; Martins, F. Human skin permeation and partition: General linear free-energy relationships analyses. *J. Pharm. Sci.* **2004**, *93*, 1508−1523.
(18) Gratton, J. A.; Abraham, M. H.; Bradbury, M. W.; Chadha, H. S. Molecular factors influencing drug transfer across the blood−brain barrier. *J. Pharm. Pharmacol.* **1997**, *49*, 1211−1216.
(19) Platts, J. A.; Abraham, M. H.; Zhao, Y. H.; Hersey, A.; Ijaz, L.; Butina, D. Correlation and prediction of a large blood−brain distribution data set. An LFER study. *Eur. J. Med. Chem.* **2001**, *36*, 719−730.
(20) Zhao, Y. H.; Le, J.; Abraham, M. H.; Hersey, A.; Eddershaw, P. J.; Luscombe, C. N.; Butina, D.; Beck, G.; Sherborne, B.; Cooper, I.; Platts, J. A. Evaluation of human intestinal absorption data and subsequent derivation of a quantitative structure−activity relationship (QSAR) with the Abraham descriptors. *J. Pharm. Sci.* **2001**, *90*, 749−784.
(21) Zhao, Y. H.; Abraham, M. H.; Le, J.; Hersey, A.; Luscombe, C. N.; Beck, G.; Sherborne, B.; Cooper, I. Rate-limited steps of human oral absorption and QSAR studies. *Pharm. Res.* **2002**, *19*, 1446−1457.
(22) Abraham, M. H.; Zhao, Y. H.; Le, J.; Hersey, A.; Luscombe, C. N.; Reynolds, D. P.; Beck, G.; Sherborne, B.; Cooper, I. On the mechanism of human intestinal absorption. *Eur. J. Med. Chem.* **2002**, 37, 595−605.
(23) Abraham, M. H.; Ibrahim, A.; Zhao, Y.; Acree, W. E., Jr. A data base for partition of volatile organic compounds and drugs from blood/plasma/serum to brain, and an LFER analysis of the data. *J. Pharm. Sci.*, in press.
(24) Abraham, M. H.; Ibrahim, A.; Acree, W. E., Jr. Air to muscle, and blood/plasma to muscle, distribution of volatile organic compounds and drugs: linear free energy analyses. *Eur. J. Med. Chem.* **2006**, *41*, 494−502.
(25) Abraham, M. H.; Treiner, C.; Rosés, M.; Ràfols, C. Linear free energy relationship analysis of microemulsion electrokinetic chromatographic determination of lipophilicity. *J. Chromatogr. A* **1996**, *752*, 243−249.
(26) Poole, S. K.; Poole, C. F. Characterization of surfactant selectivity in micellar electrokinetic chromatography. *Analyst* **1997**, *122*, 267−274.

(27) Rosés, M.; Ràfols, C.; Bosch, E.; Martínez, A. M.; Abraham, M. H. Solute−solvent interactions in micellar electrokinetic chromatography. Characterization of sodium dodecyl sulfate-Brij 35 micellar systems for quantitative structure−activity relationship modelling. *J. Chromatogr. A* **1999**, *845*, 217−226.
(28) Fuguet, E.; Ràfols, C.; Bosch, E.; Abraham, M. H.; Rosés, M. Solute−solvent interactions in micellar electrokinetic chromatography. III. Characterization of the selectivity of micellar electrokinetic chromatography systems. *J. Chromatogr. A* **2002**, *942*, 237−248.
(29) . Abraham, M. H.; Rosés, M.; Poole, C. F.; Poole, S. K. Hydrogen bonding. 42. Characterization of reversed-phase high-performance liquid chromatographic C_{18} stationary phases. *J. Phys. Org. Chem.* **1997**, *10*, 358−368.
(30) Valko, K.; Du, C. M.; Bevan, C. D.; Reynolds, D. P.; Abraham, M. H. Rapid-gradient HPLC method of measuring drug interactions with immobilized artificial membrane: comparison with other lipophilicity measures. *J. Pharm. Sci.* **2000**, *89*, 1085−1096.
(31) Lepont, C.; Poole, C. F. Retention characteristics of an immobilized artificial membrane column in reversed-phase liquid chromatography. *J. Chromatogr. A* **2002**, *946*, 107−124.
(32) Ishihama, Y.; Asakawa, N. Characterization of lipophilicity scales using vectors from solvation energy descriptors. *J. Pharm. Sci.* **1999**, *88*, 1305−1312.
(33) Abraham, M. H. Can we identify models for intestinal absorption, blood−brain barrier distribution and intestinal absorption?. In *EuroQSAR 2002. Designing Drugs and Crop Protectants: Processes, Problems and Solutions*; Ford, M., Livingstone, D., Dearden, J., Van de Waterbeemd, H., Eds.; Blackwell: Oxford, U.K., 2003; pp 5−7.
(34) Fuguet, E.; Ràfols, C.; Bosch, E.; Abraham, M. H.; Rosés, M. Selectivity of single, mixed, and modified pseudostationary phases in electrokinetic chromatography. *Electrophoresis* **2006**, *27*, 1900−1914.
(35) Lázaro, E.; Ràfols, C.; Rosés, M. Characterization of immobilized artificial membrane (IAM) and XTerra columns by means of chromatographic models. *J. Chromatogr. A* **2005**, *1081*, 163−173.
(36) Green, C. E.; Abraham, M. H.; Acree, W. E.; De Fina, K. M.; Sharp, T. L. Solvation descriptors for pesticides from the solubility of solids: diuron as an example. *Pest Manage. Sci.* **2000**, *56*, 1043−1053.
(37) Ràfols, C.; Poza, A.; Fuguet, E.; Rosés, M.; Bosch, E. Solute−solvent interactions in micellar electrokinetic chromatography: V. Factors that produce peak splitting. *Electrophoresis* **2002**, *23*, 2408−2416.
(38) Du, C. M.; Valko, K.; Bevan, C.; Reynolds, D.; Abraham, M. H. Rapid gradient RP-HPLC method for lipophilicity determination: a solvation equation based comparison with isocratic methods. *Anal. Chem.* **1998**, *70*, 4228−4234.
(39) Lombardo, F.; Shalaeva, M. Y.; Tupper, K. A.; Gao, F.; Abraham, M. H. ElogPoct: a tool for lipophilicity determination in drug discovery. *J. Med. Chem.* **2000**, *43*, 2922−2928.
(40) Du, C. M.; Valko, K.; Bevan, C.; Reynolds, D.; Abraham, M. H.; Rapid method for estimating octanol−water partition coefficient (log P_{oct}) from isocratic RP-HPLC and a hydrogen bond acidity term (A). *J. Liq. Chromatogr. Relat. Technol.* **2001**, *24*, 635−649.
(41) Valko, K.; Du, C. M.; Bevan, C.; Reynolds, D. P.; Abraham, M. H. Rapid method for the estimation of octanol/water partition coefficient (log P_{oct}) from gradient RP-HPLC retention and a hydrogen bond acidity term ($\sum\alpha_2^H$). *Curr. Med. Chem.* **2001**, *8*, 1137−1146.
(42) Poole, S.; Poole, C. F. Separation methods for estimating octanol−water partition coefficients. *J. Chromatogr. B* **2003**, *797*, 3−19.

JM0602108